ELSEVIER

Int. J. Therm. Sci. 41 (2002) 646–657

International Journal of Thermal Sciences

www.elsevier.com/locate/ijts

Enhancement of condensation heat transfer by means of EHD condensate drainage ☆

Dariusz Butrymowicz *, Marian Trela, Jarosław Karwacki

Institute of Fluid-Flow Machinery, Polish Academy of Sciences, Gen. J. Fiszera 14, PL 80-952 Gdańsk, Poland

Received 20 October 2001; accepted 8 February 2002

Abstract

The problem of electrohydrodynamic (EHD) condensation enhancement has been studied very recently. The electric field is commonly generated in such case by means of rod and mesh electrodes. The EHD method is suitable for dielectric media used in refrigeration and heat pump devices. The strong positive EHD effect has been obtained so far for vertical and horizontal bare tubes. However it was found that this effect for horizontal integral-fin tubes, commonly used in heat exchangers, is negligible small. The mechanism of the EHD condensation enhancement is discussed in the paper and a novel arrangement of the tube-electrode system is proposed. It consists of a horizontal finned tube with a rod type electrode placed beneath the tube. The experimental investigations have been carried out for this tube-electrode arrangement using HCFC-123 as a working medium. The obtained results confirmed the expectations since the application of EHD method for the new tube-electrode configuration increased the heat transfer coefficient from 27% to 110%, depending on the electrode potential. A simple model of the EHD condensate drainage has been proposed for the new tube-electrode arrangement.

Keywords: Condensation; Heat transfer enhancement; Finned tubes; Electrohydrodynamics (EHD)

1. Introduction

In many pro-ecological energy applications, suitable heat exchangers are required to combine economy with maximum possible performance. Thermal sources of renewable energy often provide low temperature levels which cannot be considered as convenient ones in respect to the cycle thermal efficiency. The other limitation of it follows from the irreversibility which occur due to the finite temperature differences in heat exchangers like as: evaporators, condensers. For example, for a heat pump the working fluid operating temperature has to be significantly higher than the heat sink in order to obtain the reasonable size of the condenser. Thus the temperature differences at the heat sink reduce the coefficient of performance COP.

For a given condenser (the heat transfer area is constant) improvement of heat transfer leads to the reduction of condensation temperature and by this means the coefficient COP may increase. On the other hand in the case when the condensation temperature is kept constant the size of the condenser may be reduced.

Fins and longitudinal drainage strips can be used in shell-and-tube condensers as the means of heat transfer augmentation [1]. The more promising way is the use of EHD enhancement technique. If it could be combined with the conventional passive enhancement (e.g. integral finning) then considerable savings in the cost of the installation might be achieved.

The paper deals with the enhancement of condensation heat transfer caused by EHD method for a novel tube-electrode configuration. The results of experimental investigations are presented for this arrangement. A simple theoretical model of EHD condensate drainage for the considered configuration is proposed.

2. EHD condensation technique

Velkoff and Miller first reported the effect of electric field on condensation heat transfer in 1965 [2]. They quoted the increase of the mean heat transfer coefficient by about

☆ This article is a follow-up to a communication presented by the authors at the ExHFT-5 (5th World Conference on Experimental Heat Transfer, Fluid Mechanics and Thermodynamics), held in Thessaloniki in September 24–28, 2001.

* Correspondence and reprints.
E-mail address: butrym@imp.gda.pl (D. Butrymowicz).

1290-0729/02/$ – see front matter
PII: S1290-0729(02)01359-5

Nomenclature

a	capillary constant $= \sqrt{\sigma/(\rho g)}$	m
A_c	cross section of the interfin channel, Eq. (9)	m^2
D_o	outer tube diameter	m
E	electric field strength	$V \cdot m^{-1}$
F	force	N
f	unit force	$N \cdot m^{-3}$
g	gravity acceleration	$m \cdot s^{-2}$
h_c	condensate layer thickness (see Fig. 11)	m
h_e	distance of the electrode from the tube bottom	m
h_f	height of condensate retention in the interfin channel (see Fig. 11)	m
H_f	height of fin	m
K_D	dimensionless tube diameter, Eq. (17a)	
K_f	dimensionless width of the interfin channel, Eq. (17b)	
$\dot{m}_w$	cooling water mass flow rate	$kg \cdot s^{-1}$
N_{eg}	dimensionless electro-gravity number	
p_e	electrical pressure, Eq. (13)	Pa
p_v	vapour pressure	Pa
P_i	perimeter along interfin channel, Eq. (7a)	m
q	electric charge density	$C \cdot m^{-3}$
R_o	outer radius of the tube	m
T_{wi}	inlet cooling water temperature	K
ΔT_c	difference between saturation temperature and outside tube wall temperature	K
U	electric potential difference between electrode and tube	V
W_b	fin spacing at fin base	m
W_t	fin spacing at fin tip	m
α	film heat transfer coefficient	$W \cdot m^{-2} \cdot K^{-1}$
β_e	ratio defined by Eq. (6)	
β_{Nu}	ratio defined by Eq. (5)	
$\bar{\delta}$	average error of the measurement of condensation heat transfer coefficient by means of Wilson plot technique	
δ_{max}	maximum error of the measurement of condensation heat transfer coefficient by means of Wilson plot technique	
γ	ratio h_c/h_e	
Γ	condensate mass flow rate	$kg \cdot m^{-1} \cdot s^{-1}$
χ	dimensionless geometrical parameter, Eq. (17c)	
χ_{de}	dimensionless electrohydrodynamic drainage parameter, Eq. (17d)	
ε	electric permittivity	$F \cdot m^{-1}$
ε_o	electric permittivity of free space $= 8.854 \times 10^{-12}$	$F \cdot m^{-1}$
ε_r	relative permittivity $= \varepsilon/\varepsilon_o$	
Φ	flooding angle, and $\Phi_f = \Phi/\pi$	rad
θ	fin tip half angle	rad
ρ	condensate density	$kg \cdot m^{-3}$
σ	surface tension	$N \cdot m^{-1}$
Ω	parameter in Eq. (4)	

Indices

b	smooth tube
c	condensation; condensate
e	electrohydrodynamic; electric
EHD	electrohydrodynamic
exp	experimental value
f	finned tube, flooding
Nu	based on the Nusselt model
T	constant temperature

200% during condensation of refrigerant R 113 on a flat, vertical plate upon the application of an intense electric field perpendicular to the plate. Experimental investigations of electrohydrodynamic (EHD) enhanced condensation heat transfer were carried out by many other researches, for example: Choi [3], Holmes and Chapman [4], Seth and Lee [5]. In all these cases, the condensation enhancement was due to an electrically induced destabilisation of the condensate film. A more recent investigation was carried out by Didkovsky and Bologa [6,7]. They obtained enhancement of condensation heat transfer as much as 20 times for the smooth vertical tube.

It should be mentioned that the most investigations have been done by application of the electric field to the vertical plates or vertical tubes [8]. The electric field is then usually generated by means of coaxial rod and mesh electrodes. The condensate is then sucked off the heat transfer area. It is worth to note that the limited data of EHD condensation enhancement exist for horizontal tubes, especially for the finned ones.

Allen and Karayiannis concluded [8], basing on their own experimental investigation, that in the case of horizontal smooth tube even the best EHD-assisted performance falls short of that given by using a single low fin profile tube without the EHD heat transfer augmentation. Thus the idea of using strong electric field to enhance heat transfer in the case of smooth horizontal tube seems to be a questionable problem. Allen and Karayiannis also claimed [8] that for the horizontal integral-fin tube with the coaxial electrode the EHD enhancement is negligibly small.

In the absence of the electric field the most important phenomenon during condensation on low profile horizontal integral-fin tube caused by the surface tension forces is called “Gregorig effect”. As it is depicted in Fig. 1(b) the liquid film at the top of the fin is convex whereas at its base is concave. Therefore the pressure within the liquid phase is

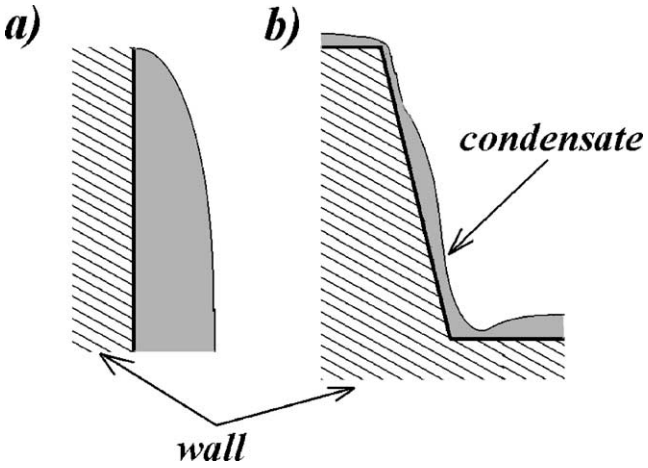

Fig. 1. The shape of the condensate film under conditions: (a) the gravity induced flow; (b) the surface tension induced flow on the fin flank—the so-called Gregorig effect.

greater at the fin top and lower at the fin base in comparison with the pressure of the vapour. This leads to the pressure gradient along the fin flank, which reduces the liquid film thickness. This is the Gregorig effect. The comparison of the shape of the condensate film flowing only under gravity and under the influence of the surface tension forces is shown in Fig. 1. Due to the Gregorig effect very high heat transfer coefficient for horizontal integral-fin tubes can be achieved.

For the case, when the strong coaxial electric field is applied to the integral-fin tube the EHD forces act against the surface tension forces, i.e., pulling out the condensate thus reducing the positive Gregorig effect. Therefore it is not surprising, as claimed by Cooper [9], that the EHD assisted condensation enhancement applied to the horizontal integral-fin tube is negligible. It should be stressed here that this conclusion is valid only for the cases when the coaxial electric field caused by coaxial wires or coaxial mesh electrode system are applied. The above considerations shed more light on the EHD condensation mechanism and are very helpful in the formulation of a new active method for EHD enhancement of condensation on a horizontal integral-fin tube. This method is presented in this paper.

3. Mechanism of EHD condensation enhancement

The physical basis of the electrically enhanced condensation is due to the EHD force f_e generated by an electric field. It is given by equation [8]:

$$f_e = qE - \frac{1}{2}E^2\nabla\varepsilon + \frac{1}{2}\nabla\left[E^2\left(\frac{\partial\varepsilon}{\partial\rho}\right)_T\rho\right] \tag{1}$$

It may be further written in a more detail form for non-polar fluids [10] as:

$$\begin{aligned} f_e &= f_1 + f_2 + f_3 + f_4 \\ &= qE - \frac{1}{2}E^2\nabla\varepsilon + \frac{1}{6}\varepsilon_o(\varepsilon_r - 1)(\varepsilon_r + 2)\nabla E^2 \\ &\quad + \frac{1}{6}\varepsilon_o E^2\nabla\left[(\varepsilon_r - 1)(\varepsilon_r + 2)\right] \end{aligned} \tag{2}$$

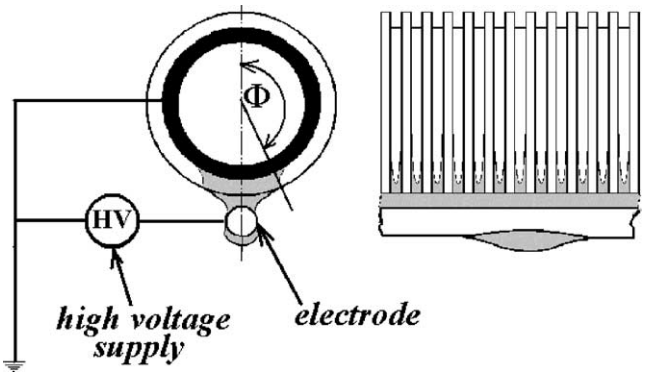

Fig. 2. The idea of proposed EHD condensate drainage.

The first component represents the electrophoretic force f_1 exerted by an electric field upon electric charges in the fluid. The second component f_2, comes from the spatial distribution of electric permittivity ε, which are not caused by electrostriction. This component acts perpendicularly to the inter-phase surface from the material of higher permittivity (liquid) to the material of lower permittivity (vapour). This component acts to disturb the condensate film. The third component f_3 is the dielectrophoretic force which is due to the non-uniformity of the electric field. This force pushes condensate towards higher electric field strength. The last component f_4 is the electrostriction force which occurs whether or not an applied field is uniform. This force depends on non-uniformity of electrical permittivity. In the case of film condensation this component is significant at the inter-phase surface only when abrupt change of ε_r occurs. The direction of this force is the same as direction of increasing permittivity (from vapour to liquid) and perpendicular to the inter-phase surface.

For the proper tube-electrode arrangement, a significant area of the tube surface remains unflooded due to the condensate flow induced by the EHD forces, thus making favourable conditions for the condensate heat transfer. In other word the proper application of the EHD condensate drainage shell lead to an increase of the so-called flooding angle Φ_f, a parameter which clearly define the area of the finned tube free from the condensate.

4. Proposed EHD condensate drainage method

In this paper a new active method of augmentation of condensation heat transfer by means of EHD condensate drainage is proposed. The idea of this method is illustrated in Fig. 2. The tube-electrode system consists of a horizontal finned tube and a rod-type electrode placed beneath the tube. In this case the electric field is generated between the electrode and only the lower part of the finned tube. The major roles play in such case the components f_2 and f_4 of the EHD force.

Therefore, taking into account the EHD mechanism one may expect that the majority of the tube surface is not affected by the electric field with the exception of the small part of it at the tube bottom. This part usually plays a minor role in heat transfer also without the electric field since the interfin spaces are usually flooded totally by the condensate. Thus for the considered case we have two positive phenomena in respect to the heat transfer augmentation. The first one follows from the Gregorig effect which takes place in the upper part of the tube (not disturbed by the EHD forces) and second one is due to the EHD forces pulling down the condensate from the bottom of the tube. It is seen that in this method the EHD forces act only on the condensate drainage process and not on the condensation phenomenon itself. This feature express the main difference between the old methods of the EHD enhancement and the new one proposed here.

The important parameter describing the condensate retention between the fins is the so-called flooding angle Φ (see Fig. 2) which is the angle measured from the top of the tube to the position where entire fin flanks and the interfin space are blanked by retained condensate. It has been proved by Webb et al. [11] that the heat transfer rate across the condensate retained zone is less than 1% of the total heat transfer rate for the whole tube for most of the refrigerants. The dimensionless form of the flooding angle can be calculated from the formula developed by Honda [12]:

$$\Phi_{\mathrm{f}} = \frac{1}{\pi}\arccos\left(4\frac{a^2}{W_{\mathrm{t}}D_{\mathrm{o}}}\cos\theta - 1\right) \tag{3}$$

The present authors showed [13], that the majority of the theoretical models of condensation heat transfer coefficient on horizontal integral-fin tubes can be described by the general formula:

$$\alpha_{\mathrm{f}} = \alpha_{\mathrm{b}}\Omega\Phi_{\mathrm{f}} \tag{4}$$

where Ω is a parameter taking into account a combined product of the heat transfer area ratio as well as fin efficiency, and α_{b} is the Nusselt type heat transfer coefficient for the bare tube. In this equation α_{f} is referred to the envelope surface area of diameter D_{o}. Both coefficients are referred to the same temperature difference ΔT_{c}. According to the above formula the heat transfer coefficient is proportional to the flooding angle Φ_{f}.

5. Apparatus and procedure

The main goal of the experimental investigation was to provide the data, which could confirm the usefulness of the proposed tube-electrode arrangement (Fig. 2) in respect to the EHD condensation enhancement.

The experimental investigation was conducted on the test rig depicted in Fig. 3. It covered measurements of the heat transfer coefficient during condensation of refrigerant HCFC-123 at the average saturation temperature $+40\,^{\circ}\mathrm{C}$. The rig consisted of two main elements—the condenser 1 with a tested tube 2 mounted inside it and a vapour generator 12. The length of the testing section was 1.0 m. The condenser was equipped with six glass windows so the observation of the condensate flow pattern was possible. Other elements of the condenser were: a dish 4 to collect the condensate, a gear 6 to lift the drainage electrode, vapour supplying tube 7 and air purging valve 18. Thanks to the lifting gear the electrode could be fitted at any distance from the tested tube. The test rig was equipped with a calibrating tank 10 to measure the condensate flow rate and dehydrator 9 filled with molecular sieves of type 4A. Only the liquid leaving the tested tube could flow down to these tanks, the remaining condensate flowed down through another separate pipeline 8 to the vapour generator 12 placed in a hot water vessel 13 equipped with four heaters. The high potential was supplied to the electrode by sparking plug mounted at the backside of the condenser. A detailed description of the rig is described in [14].

The following quantities were measured in the course of the investigations:

- inlet water temperature measured in tank 17 and at the beginning of the test section,
- outlet water temperature measured in tank 17 and at the end of the test section,
- vapour temperature measured at two points inside condenser,
- vapour pressure measured by the use of the mano-vacuummeter with accuracy class of 0.6,
- vapour pressure measured by the use of the pressure transducer with accuracy class of 0.1,
- water flow rate measured by the use turbine flowmeter with accuracy class of 1.0,
- volume of condensate in calibrating tank 10,
- time of filling up the tank 10.

All temperatures were measured by means of thermocouples of the type K with the use of the acquisition data system. The temperature measurement error was ± 0.15 K.

The data were recorded once a steady state was achieved. Basically from all data points the only ones were taken into account when the difference of the heat flux calculated from the heat balances on water as well as on the vapour sides did not exceed 15%. For 44% of data points this difference was below 5%.

The condensation heat transfer coefficient was determined by means of Wilson plot technique very similar to those one modified by Briggs and Young [15]. It is referred to the envelope surface area of diameter D_{o}. The details of the methodology of determination of heat transfer coefficient are presented in [16].

The dimensions of the investigated tubes are given in Table 1. The brass rod-type electrode of the outer diameter 5.0 mm was used. The measurements covered the cooling

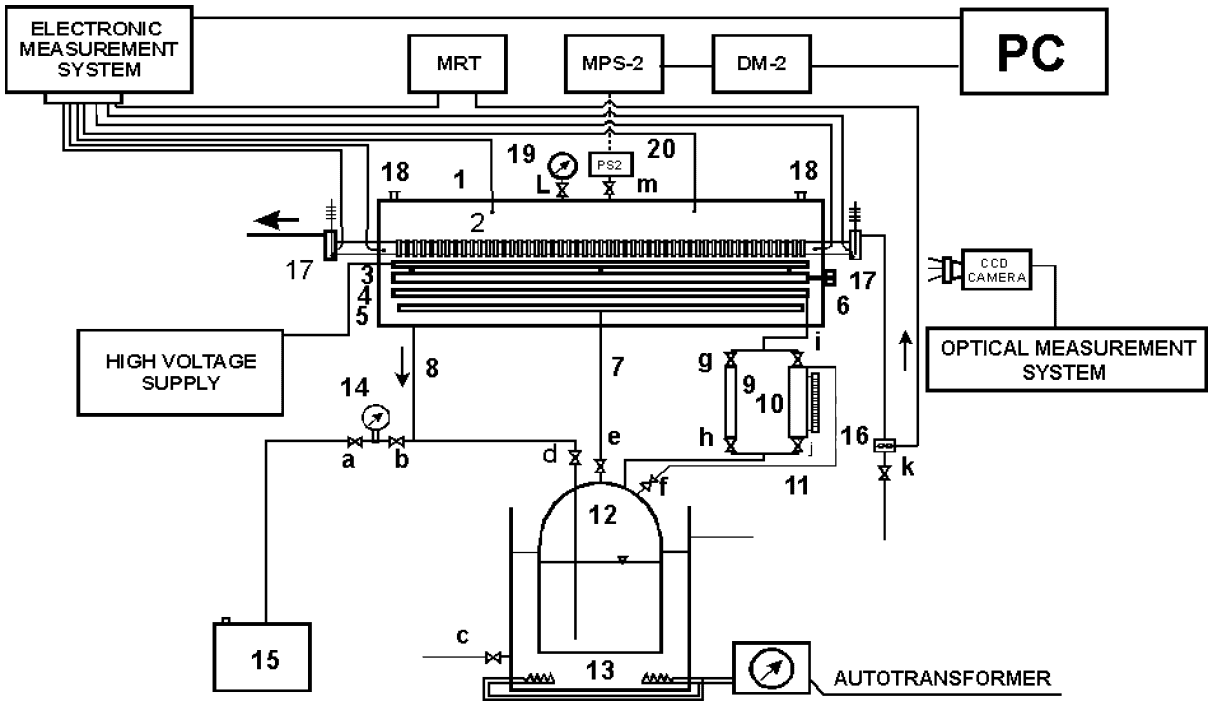

Fig. 3. The schematic diagram of the testing rig: 1—condenser, 2—tested tube, 3—electrode, 4—condensate dish, 5—vapour distributor, 6—electrode mechanism, 7—vapour supplying tube, 8—condensate outflow, 9—dehydrator, 10—condensate calibrating tank, 11—levelling line, 12—vapour generator, 13—hot water vessel, 14—vacummeter, 15—vacuum pump, 16—turbine water flow rate meter, 17—water temperature measurement tank, 18—air purging valve, 19—mano-vacuum meter, 20—pressure sensor, DM-2—electronic multi-manometer, MRT—digital encounter.

Table 1
Geometry of the tested tubes

Tube	Unit	1	2	3	4	5	6
fin density	m^{-1}	bare	1026.7	bare	740	bare	1851.7
inter diameter	mm	13.0	11.02	15.60	13.80	13.0	13.0
fin root diameter	mm	–	13.42	–	16.00	–	15.2
outer diameter	mm	16.0	16.17	18.76	18.76	16.0	16.0
fin pitch	mm	–	0.97	–	1.35	–	0.54
fin height	mm	–	1.38	–	1.50	–	0.40
fin thickness at fin root	mm	–	0.40	–	0.46	–	0.27
fin thickness at fin top	mm	–	0.21	–	0.29	–	0.27
heat transfer area ratio	–	–	3.31	–	3.52	–	2.42
material		cooper	cooper	nickeline	nickeline	brass	brass

water flow rate within the range 3.7–13.0 $l \cdot min^{-1}$ for each test tube.

6. Experimental results

The investigation covered the measurement of heat transfer coefficient for the finned tubes and for the smooth ones for the reference. The average and maximum errors δ of the measurement of the condensation heat transfer coefficient by means of Wilson plot technique are given in Table 2. Details concerning the calculation of the measurement error are presented in [16].

The experimental data of heat transfer coefficient were compared to ones given by the Nusselt theory. Two enhancement factors β_{Nu} and β_e were introduced in the analysis. They are also given in Table 2:

(a) the ratio β_{Nu} is referred to the Nusselt model for the smooth horizontal tube:

$$\beta_{Nu} = \frac{\alpha_{exp}}{\alpha_{Nu}} \tag{5}$$

(b) the ratio β_e is referred to the measured value of heat transfer coefficient in the absence of electric field:

$$\beta_e = \frac{\alpha_{exp}}{\alpha_{exp,U=0}} \tag{6}$$

The experimental results of the condensation of refrigerant HCFC-123 for tubes No. 1 and No. 2 (of OD 16 mm) are presented in Fig. 4. It is seen that the heat transfer coefficient for the finned tube increased by 240% in comparison

Table 2
Results of condensation heat transfer measurement

Tube	U [kV]	h_e [mm]	β_{Nu}	β_e	$\bar{\delta}$ [%]	δ_{max}
No. 1	0	9.5	1.09	1.00	6.2	7.5
No. 2	0	9.5	3.71	1.00	10.8	11.2
	25	9.5	4.71	1.27	9.9	10.1
No. 3	0	8.6	0.98	1.00	9.6	11.0
No. 4	0	8.6	2.64	1.00	15.4	16.2
	22	8.6	5.48	2.08	9.6	9.8
No. 5	0	6.0	1.097	1.00	6.5	7.6
No. 6	0	6.0	2.526	1.00	6.8	7.1
	0	9.5	2.731	1.00	5.7	6.2
	22	9.5	3.449	1.26	6.2	6.6
	25	6.0	2.593	1.03	6.1	6.6
	27	9.5	3.382	1.24	12.9	13.5

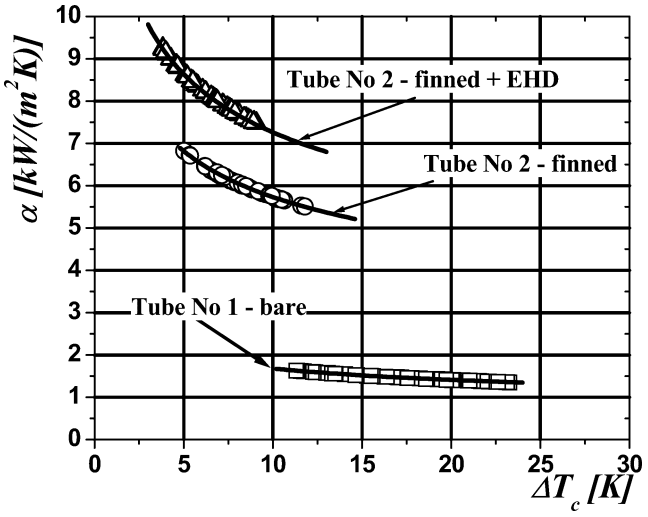

Fig. 4. Results of the experimental investigations of tube No. 1 and No. 2, $U = 25$ kV.

with the bare one in the absence of the electric field (see the two lower curves). The application of the voltage of 25.0 kV caused the further increase of the condensation heat transfer coefficient by 27%. The total increase of the heat transfer coefficient in comparison with the bare tube was found to be 330%.

The observation of the condensation phenomenon proved that the condensate was almost completely removed from the interfin channel (see Fig. 7(c)). In this case the value of the flooding angle was $\Phi_{fe} \approx 1.0$. The theoretical value of the flooding angle calculated from Eq. (3) gives $\Phi_f = 0.74$ and estimated value from the photograph was equal to $\Phi_f = 0.78$. Basing on these results and Eq. (4) one can estimate theoretical increase of the condensation heat transfer coefficient due to elimination of condensate retention as $\alpha_{fe}/\alpha_f = \Phi_{fe}/\Phi_f = 1.00/0.78 = 1.28$ which agrees very well with the experimental results.

The experimental results obtained for tube No. 3 and No. 4 (i.e., tubes having OD 19 mm) are presented in Fig. 5. It is seen that the heat transfer coefficient for the finned tube increased by 170% in comparison with the bare one. The application of the voltage of 22.0 kV caused the

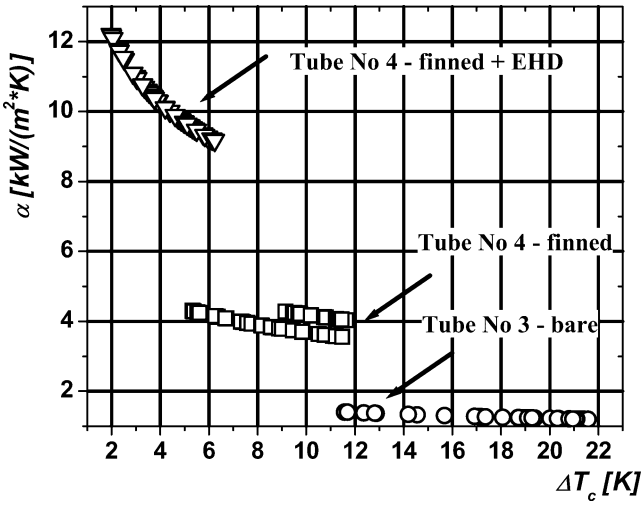

Fig. 5. Results of the experimental investigations of tube No. 3 and No. 4, $U = 22$ kV.

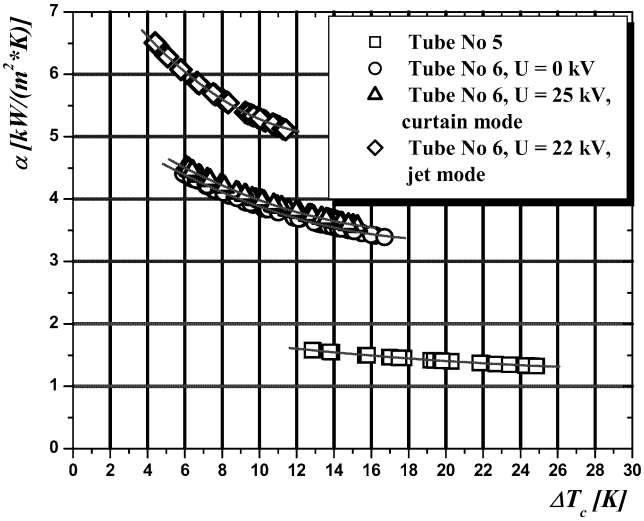

Fig. 6. Results of the experimental investigations of tube No. 6 and No. 5.

further increase of the condensation heat transfer coefficient by 110%. This is the very impressive result. The total increase of the heat transfer coefficient (due to the finning and EHD effects) in comparison with the bare tube was found to be 460%.

In spite of a relatively very high fin density of the tube No. 6 (Fig. 6), the surface area increase for it was low due to the very low height of fins. Therefore there is no surprise that the heat transfer enhancement due to the finning in the absence of electric field was only 160% in comparison with the bare tube of the same outer diameter and made of the same material (i.e., tube No. 5). The EHD heat transfer enhancement at voltage $U = 22$ kV was found to be 26% higher in comparison with the same finned tube but without EHD. It was very interesting that no heat transfer enhancement was found at higher voltage $U = 27$ kV. This effect may be explained mainly by the fact that for this case the condensate flowed out from the tube bottom in the form

of a liquid sheet (curtain). The liquid sheet appears here as a not favourable flow pattern. For the first case ($U = 22$ kV) the jet mode was observed, not the curtain one. The results proved that heat transfer enhancement strongly depends on the condensate flow pattern. This problem will be discussed below in more details.

It is worth to note that the experimental data shown in Figs. 4, 5, 6 was obtained at the same range of the cooling water flow rate $\dot{m}_w$, the same inlet water temperature T_{wi} and the vapour pressure p_v for all tubes used. This means that the first (or last) data point for one tube corresponds to the first (or last) data point for the other tube. It is seen from Figs. 4, 5, 6 that the increase of heat transfer coefficient was accompanied by the decrease of the temperature difference ΔT_c.

The comparison of the heat transfer enhancement for different tube geometry and supplied voltage should be done keeping contact values of $\dot{m}_w$, T_{wi}, and p_v instead for given ΔT_c, as it is commonly applied in the literature. It is evident that for the first approach the real increase in heat transfer coefficient is much higher than for the second one.

It can be seen from Figs. 4, 5, 6 that the temperature difference ΔT_c may be reduced as much as three times for the EHD condensation enhancement for tube No. 2, almost six times for tube No. 4 and almost two times for tube No. 6 in comparison with the smooth tubes of the same diameter. Since for the thermodynamic cycles the temperature difference ΔT_c in the condenser may be considered as a part of the total temperature difference between the heat source and the heat sink then the significant decrease of ΔT_c due to the heat transfer enhancement by the considered method leads to the strong increase of the cycle efficiency. It is easy to show that this effect of improvement is more significant for the refrigeration cycles where the temperature difference between the heat source and the sink is relatively small.

Generally, the experimental data obtained for the proposed tube-electrode configuration proved it superiority over the coaxial rod and mesh electrode system. The improvement of heat transfer is significant here and not negligibly small as claimed by Allen and Karayiannis [8] for the second system.

7. Condensate flow patterns

The experimental investigation proved that a very important role in the EHD condensation enhancement plays the flow pattern of the condensate leaving the tube. The condensate flow patterns occurred for tube No. 2 and No. 4 are shown in Figs. 7 and 8, respectively. They were the same for the given range of the condensate mass flow rate and the applied voltage.

It is very important to note, that the condensate flow patterns observed for Tube No. 2 (see Fig. 7(d)) were slightly different in comparison with Tube No. 4 (see Fig. 8(d)). In the latter case the condensate jets were formed from each fin tip. Therefore the jet spacing was the same as the fin pitch. In the case of Tube No. 2 the jet spacing was as much as 3.0–5.0 mm, i.e., it was sufficiently larger than fin pitch. This may be attributed as the main reason for such significant improvement of condensation heat transfer measured for Tube No. 4.

The general schematic diagram of the flow patterns of the condensate leaving the tube at applied voltage is presented in Fig. 9. Four distinguished modes were observed during the experimental investigation: drop, jet, cone and curtain mode. The drop mode occurred in the absence of the electric field. For a medium voltage range the flow pattern changed from drop to jet and next to jet-cone modes with increasing the voltage. It is interesting to note that in the jet-cone mode very complex condensate flow occurs. There is a vertical downward flow in the jets accompanied by the stagnation of the condensate in the cones. As the voltage further increased, the cones became thicker (see Fig. 9(c), 9(d) and 9(e)) what widen the condensate stagnation zones and weaken the drainage process. Finally, as the voltage is high enough the curtain mode occurs (Fig. 9(f)) which almost stop the drainage process from the tube. This is the worst condensate flow pattern observed in these experiments.

One may expect that the boundaries between the flow patterns depend not only on the applied voltage but also on the electrode type, it distance to the tube and the properties of the working fluids. This problem needs further more complex investigation.

8. Modelling of EHD condensate drainage

The experimental data obtained for the EHD condensate drainage applied to the proposed in Fig. 2 tube-electrode configuration confirmed it advantage and superiority over the other ones. It appeared that for the configuration used, the EHD method caused significant increase in heat transfer. This result is very promising and encouraging to take an attempt to develop a theoretical model of the phenomenon. The problem of condensation heat transfer on the finned tube under the action of gravity and the electric field forces is very complex. Thus one has to start first with a very simple model. Such model is presented below. The following simplifications are made in the analysis:

- The heat transfer enhancement occurs due to reduction of condensate retention (see the formula (4)). The condensate retention is described by the flooding angle Φ and its corresponding height of retained condensate level h_f (see Fig. 10).
- The effect of the tube curvature on the condensate retention as well as on the distribution of the electric field is neglected so the vertical finned plate replaces the horizontal finned tube in respect to heat transfer in the model as it is depicted in Fig. 11. (It is worth to note

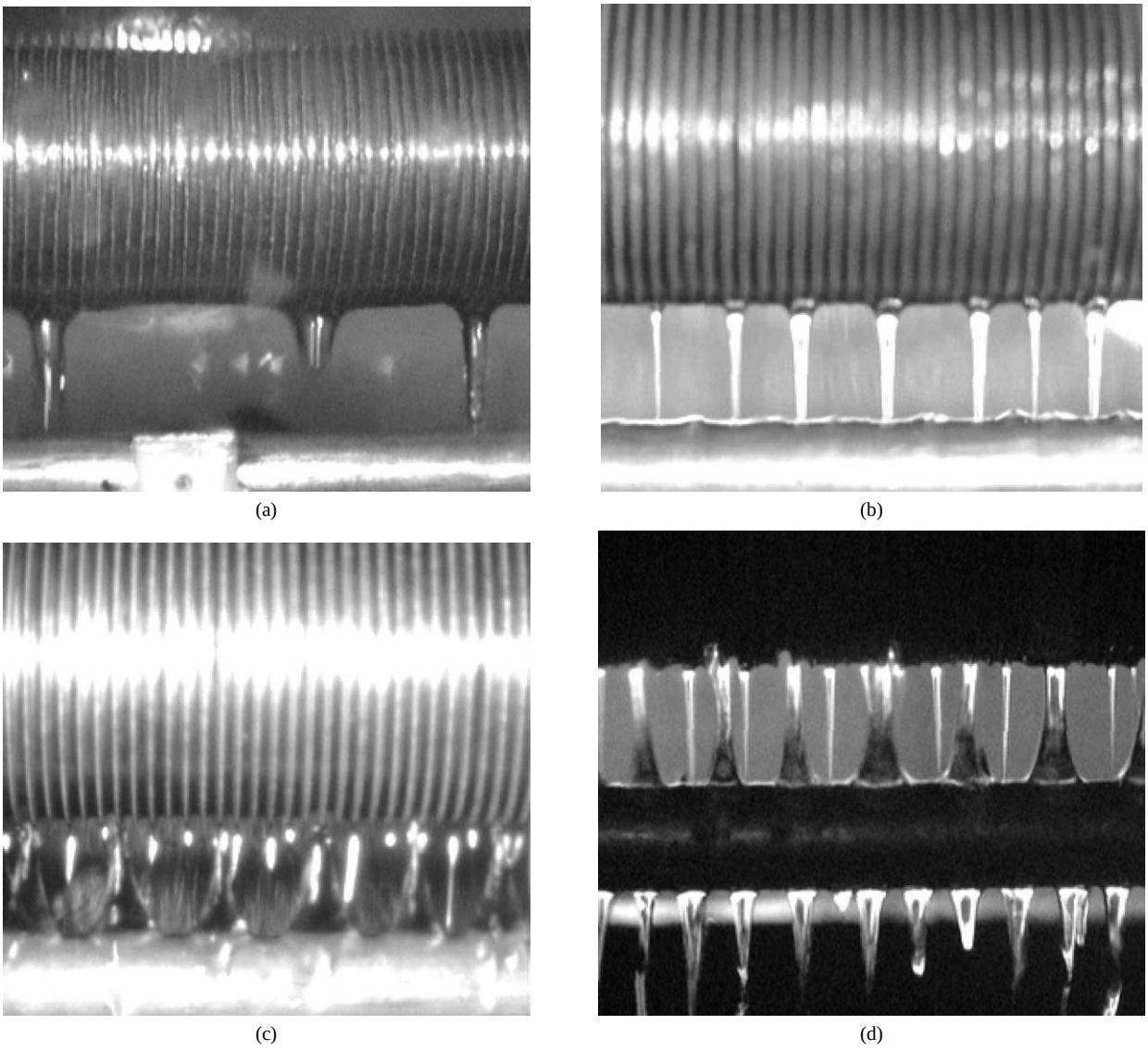

Fig. 7. The condensate flow pattern from tube No. 2: for $U = 0$: $\Gamma = 9.5$–19.3×10^{-3}kg·m^{-1}·s^{-1}, for $U = 10$ kV: $\Gamma = 11.4$–22.7×10^{-3} kg·m^{-1}·s^{-1}, for $U = 15$ kV: $\Gamma = 11.6$–22.2×10^{-3} kg·m^{-1}·s^{-1}. (a) $U = 0$ kV, droplet mode; (b) $U = 10$ kV, jet mode; (c) $U = 15$ kV, jet-cone mode; (d) $U = 15$ kV, jet-cone mode, silhouette.

that experimental investigations of Rudy and Webb [17] obtained under gravity and surface tension forces only revealed that the height of the retained condensate levels for both finned vertical plate and the horizontal finned tube of the same fin geometry are the same).

- The distance h_e between the electrode and tube bottom as well as fin density are sufficiently large to treat the tube bottom as a smooth metal surface.
- The electric field in the space between the electrode and the very bottom of the tube is uniform.
- The condensate flowing from the bottom of the tube forms the condensate layer of the average substitute thickness h_c. The thickness h_c depends on the condensate flow pattern.

Lets consider the forces acting on the condensate retained in the interfin channel on the vertical finned plate as it is depicted in Fig. 11. The surface tension force F_1 acts upward and its value is given by the following formula:

$$F_1 = \sigma P_i \tag{7}$$

where P_i is a perimeter along the interfin channel. For the integral fins P_i can be written as:

$$P_i = 2\frac{H_f}{\cos\theta} + W_b \tag{7a}$$

The second surface tension force F_2 acts downwards and its value is simply given by the formula:

$$F_2 = \sigma W_t \tag{8}$$

The gravity force is easy to calculate since:

$$F_g = \rho g V_c = \rho g A_c h_f \tag{9}$$

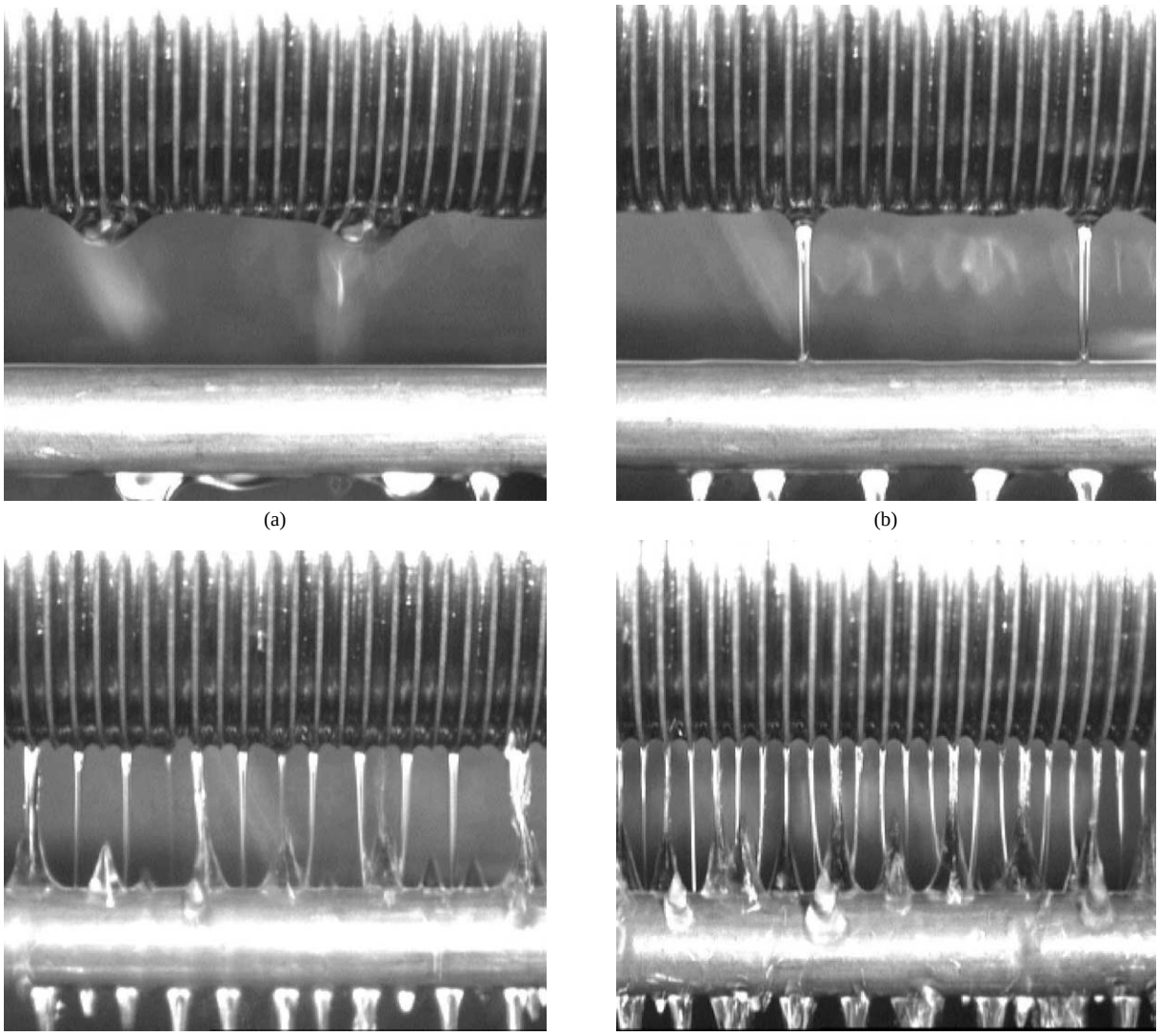

Fig. 8. The condensate flow pattern from tube No. 4, for $U = 0$: $\Gamma = 7.0\text{–}14.6 \times 10^{-3}$ kg·m^{-1}·s^{-1}, for $U = 22$ kV: $\Gamma = 7.5\text{–}18.3 \times 10^{-3}$ kg·m^{-1}·s^{-1}. (a) $U = 0$ kV, droplet mode; (b) $U = 6$ kV, jet mode; (c) $U = 16$ kV, jet-cone mode; (d) $U = 22$ kV, jet-cone mode.

where c is the volume of retained condensate between the adjacent fins and A_c is the cross section of the interfin channel:

$$A_c = \frac{1}{2} H_f (W_b + W_t) \tag{9a}$$

The electrohydrodynamic force F_{EHD} acts downwards so the following force balance equation can be written:

$$F_1 - F_g - F_2 - F_{EHD} = \sigma P_i - \rho g A_c h_f - \sigma W_t - F_{EHD} = 0 \tag{10}$$

From Eq. (10) one can calculate the height of the condensate retention in the interfin channel:

$$h_f = \frac{\sigma (P_i - W_t) - F_{EHD}}{\rho g A_c} \tag{11}$$

In order to calculate the electrohydrodynamic force F_{EHD}, one can consider the theoretical horizontal capacitor (see Fig. 11) of the thickness h_e, part of which is occupied by the liquid layer of the thickness h_c with a relative electric permittivity $\varepsilon_r = \varepsilon_c$. The rest space of the capacitor is occupied by the vapour with relative dielectric permittivity equal to unity: $\varepsilon_r = 1$. The electric field for such capacitor may be calculated from the well-known formula:

$$E = \frac{U}{h_e} \left[\frac{h_c}{h_e} + \varepsilon_c \left(1 - \frac{h_c}{h_e} \right) \right]^{-1} \tag{12}$$

It could be showed [18] that in the considered capacitor the action of all components of the electrohydrodynamic force is equivalent to the so-called electric pressure, which acts within the liquid phase:

$$p_e = \frac{\varepsilon_o \varepsilon_c (\varepsilon_c - 1)}{2} E^2 \tag{13}$$

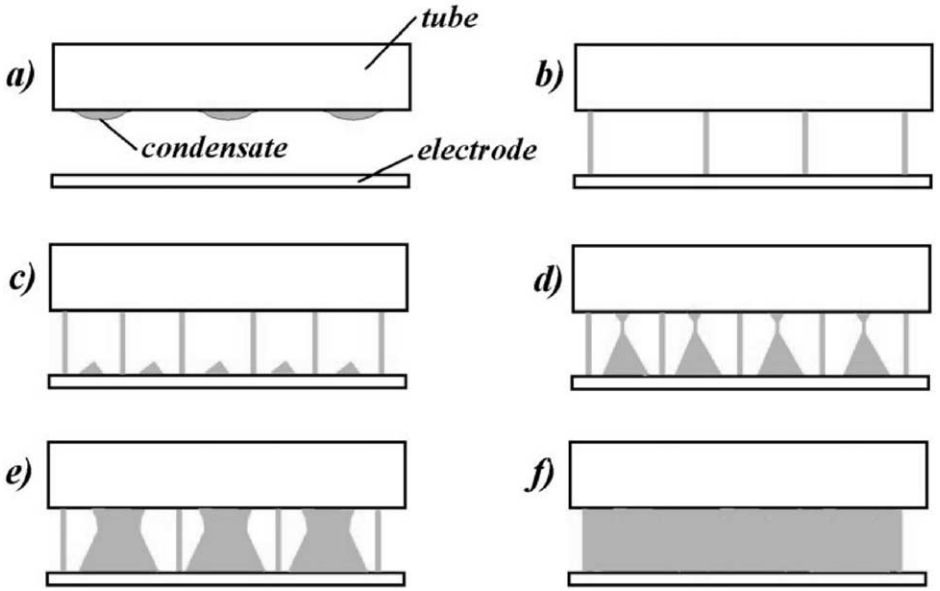

Fig. 9. Schematic diagram of flow patterns of condensate leaving the tube—the effect of increase of the electrode potential: (a) drop mode; (b) jet mode; (c), (d), (e) jet-cone mode; (f) curtain mode.

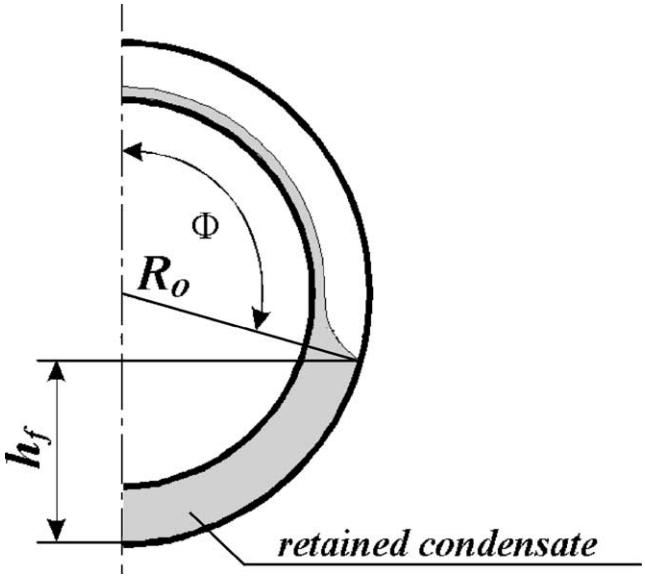

Fig. 10. Sketch of the condensate retention on a horizontal finned tube.

From Eq. (13) one can calculate then the electrohydrodynamic force acting on the condensate in the interfin channel:

$$F_{\mathrm{EHD}} = p_{\mathrm{e}} A_{\mathrm{c}} \tag{14}$$

From Eqs. (9a), (11), (12) and (13) it is easy to obtain the formula for the height of the condensate retention in the interfin channel:

$$h_{\mathrm{f}} = 2\frac{a^2}{W_{\mathrm{t}} - H_{\mathrm{f}}\,\mathrm{tg}\,\theta}\frac{1-\sin\theta}{\cos\theta} - \frac{p_{\mathrm{e}}}{\rho g} \tag{15}$$

Having the height h_{f} one can simply calculate the flooding angle (see Fig. 10):

$$\Phi = \arccos\left(\frac{h_{\mathrm{f}}}{R_{\mathrm{o}}} - 1\right) \tag{16}$$

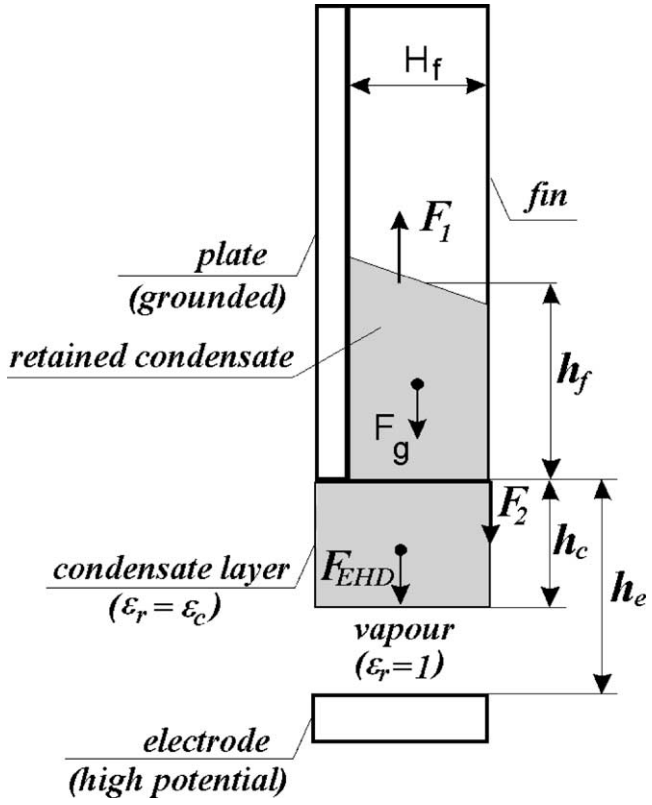

Fig. 11. Physical model of EHD condensate drainage.

Lets introduce now the following dimensionless quantities:

(a) dimensionless tube diameter:

$$K_{\mathrm{D}} = \frac{D_{\mathrm{o}}}{2a} \tag{17a}$$

(b) dimensionless width of the interfin channel:

$$K_f = \frac{W_t - H_f \operatorname{tg}\theta}{2a} \frac{\cos\theta}{1-\sin\theta} \tag{17b}$$

(c) geometrical parameter:

$$\chi = (K_D K_f)^{-1} \tag{17c}$$

(d) parameter of the electrohydrodynamic drainage:

$$\chi_{de} = \frac{1}{2}\frac{N_{eg}}{K_f} \tag{17d}$$

where the dimensionless electro-gravity number is given by:

$$N_{eg} = \frac{\varepsilon_o \varepsilon_c (\varepsilon_c - 1) E^2}{\rho g a} \tag{17e}$$

Eq. (17e) could be written with the help of Eq. (12) as:

$$N_{eg} = \frac{\varepsilon_o \varepsilon_c (\varepsilon_c - 1)}{\rho g a} \left(\frac{U}{h_e}\right)^2 \left[\gamma + \varepsilon_c (1-\gamma)\right]^{-2} \tag{18}$$

where: $\gamma = h_c/h_e$. Then the final formula for dimensionless flooding angle could be written as:

$$\Phi_{fe} = \frac{1}{\pi} \arccos\left[\chi(1-\chi_{de}) - 1\right] \tag{19}$$

Having had the flooding angle for the condensation on the finned tube under the action of EHD drainage one can easily obtain the heat transfer coefficient for this situation. It may be calculated with the help of Eq. (4) for the given fin geometry with $\Phi_f = \Phi_{fe}$.

The simple analytical model presented above clearly indicates the influence of the flow pattern on the flooding angle Φ_f and by it on the heat transfer coefficient α_f. This influence is expressed by the ratio $\gamma = h_c/h_e$ which appears in Eqs. (17d), (17e) and (18). The value of it depends on the condensate flow pattern and may be at present calculating with the help of the experimental data only. Two limiting values of γ may be easily established. The first one appears when the condensate is absent at the tube bottom. Then, according to Fig. 11, $h_c = 0$ and $\gamma = 0$. The second limiting value of γ is connected with the curtain mode of the condensate leaving the tube (see Fig. 9(f)). When the flow pattern approaches the curtain mode then $h_c \to h_e$ and $\gamma \to 1$. But at $\gamma = 1$ we have singularity because all the assumptions of the model fail. For this case the interfacial surface disappears since the whole tube-electrode space is filled with the condensate.

The present authors measured [19] the relative permittivity of the refrigerant HCFC-123 and obtained the value $\varepsilon_c = 4.7$. On the basis of the measured heat transfer coefficient α_f with the use of Eq. (4) and the above model Eq. (19) one can calculate the ratio $\gamma = h_c/h_e$. It takes the values $\gamma = 0.251$ and $\gamma = 0.443$ for the tubes No. 2 and No. 6, respectively. These values of γ correspond to the jet mode of the condensate leaving the tube. For the time being it seems that this mode is the most favourable one for EHD condensate drainage.

9. Conclusions

The experimental results obtained for the EHD condensate drainage applied to the novel tube-electrode arrangement shown in Fig. 2, confirmed it advantage and superiority over the other ones.

The effectiveness of this method depends on the geometry of the tube as well as on the applied electrode potential. The enhancement of heat transfer coefficient ranges from approximately 30% for tube No. 2 and tube No. 6 to 110% for tube 4. The total increase of the heat transfer coefficient in comparison with the bare tube (without the electric field) was found to be 330% and 460% for tube No. 2 and No. 4, respectively.

The average temperature difference between condensing vapour and outside tube wall for finned tube applied with the EHD condensate drainage was reduced as much as two to six times for tube No. 6 and No. 4, respectively in comparison with the bare one without the EHD effect.

The simple analytical model of the EHD condensate drainage from the horizontal finned tube has been proposed. It involves among others the influence of the condensate flow pattern on the heat transfer coefficient expressed by the ratio $\gamma = h_c/h_e$. Two limiting cases of this ratio were evaluated. The intermediate values of it have to be established basing on the experimental data.

The process of condensation heat transfer on horizontal finned tube in the electric field is very complex, so many aspects of it need further examinations. One of them concerns the optimal geometry of the tube-electrode configuration.

References

[1] M. Trela, D. Butrymowicz, Enhancement of condensate drainage from a horizontal integral-fin tube by means of a solid strip, Internat. J. Heat Mass Transfer 42 (18) (1999) 3447–3459.

[2] H.R. Velkoff, J.H. Miller, Condensation of vapor on a vertical plate with a transverse electrostatic filed, Trans. ASME J. Heat Transfer (1965) 197–201.

[3] H.Y. Choi, Electrohydrodynamic condensation heat transfer, Trans. ASME J. Heat Transfer (1968) 98–102.

[4] R.E. Holmes, A.J. Chapman, Condensation of Freon-114 in the presence of a strong nonuniform alternating electric field, Trans. ASME J. Heat Transfer (1970) 616–620.

[5] A.K. Seth, L. Lee, The effect of an electric field in the presence of noncondensable gas on film condensation heat transfer, Trans. ASME J. Heat Transfer (1974) 257–258.

[6] A.B. Didkovsky, M.K. Bologa, Vapour film condensation heat transfer and hydrodynamics under the influence of an electric field, Internat. J. Heat Mass Transfer 24 (5) (1981) 811–819.

[7] M.K. Bologa, V.P. Korovkin, I.K. Savin, Mechanism of condensation heat transfer enhancement in an electric field and the role of capillary processes, Internat. J. Heat Mass Transfer 38 (1) (1995) 175–182.

[8] P.H.G. Allen, T.G. Karayannis, Electrohydrodynamic enhancement of heat transfer and fluid flow, Heat Recovery Syst. CHP 15 (5) (1995) 389–423.

[9] P. Cooper, Practical design aspects of EHD heat transfer enhancement in evaporators, ASHRAE Trans. 98 (2) (1992) 445–454.

[10] Z. Yu, R.K. Al-Dadah, R.H.S. Winterton, A theoretical investigation of electrohydrodynamically (EHD) enhanced condensation heat transfer, in: Proc. of Internat. Conf. Two-Phase Modelling and Experimentation, Pisa, Italy, Vol. 1, 1999, pp. 463–472.
[11] R.L. Webb, T.M. Rudy, M.A. Kedzierski, Prediction of the condensation coefficient on horizontal integral-fin tubes, Trans. ASME J. Heat Transfer (1985) 369–376.
[12] H. Honda, S. Nozu, K. Mitsumori, Augmentation of condensation on horizontal finned tubes by attaching a porous drainage plate, in: Y. Mori, W.-J. Yang (Eds.), Proceedings of ASME–JSME Thermal Engineering Joint Conference, Vol. 3, 1983, pp. 289–296.
[13] D. Butrymowicz, M. Trela, Investigations of heat transfer on a horizontal fin-tube fitted with the drainage strip, Archiv. Thermodynam. 18 (3–4) (1997) 25–48.
[14] D. Butrymowicz, Testing rig for investigation of condensation on single horizontal tube, Internal Report of the Institute of Fluid-Flow Machinery, archive No 437/99, Gdańsk, 1999 (in Polish).
[15] D.E. Briggs, E.H. Young, Modified wilson plot techniques for obtaining heat transfer correlations for shell and tube heat exchangers, Chem. Engrg. Progr. Sympos. Ser. 92 (65) (1969) 35–45.
[16] D. Butrymowicz, Indirect method of measurement of condensation heat transfer coefficient for horizontal tube, Internal Report of the Institute of Fluid-Flow Machinery, archive No 497/99, Gdańsk, 1999 (in Polish).
[17] T.M. Rudy, R.L. Webb, An analytical model to predict condensate retention on horizontal integral-fin tubes, Trans. ASME J. Heat Transfer 107 (1985) 361–368.
[18] D. Butrymowicz, J. Karwacki, M. Trela, Investigations of condensation on horizontal tubes under conditions of electrohydrodynamic condensate drainage, Scientific Notes of the Institute of Fluid-Flow Machinery of Polish Academy of Sciences, No 523/1482/2002, Gdańsk, 2002 (in Polish).
[19] J. Karwacki, M. Lackowski, D. Butrymowicz, Measurement of electric permittivity of freons, Report of the Institute of Fluid-Flow Machinery of Polish Academy of Sciences, No. 286/2000, Gdańsk, Poland, 2000 (in Polish).